

Field Measurements of Nonlinear Distortion in Digital Cable Plants

Tom Williams and Belal Hamzeh, CableLabs
Ron Hranac, Cisco Systems

Abstract

As cable networks transition from the carriage of analog TV signals to digital signals, the second- and third-order nonlinear distortion products, known as composite second order (CSO) and composite triple beat (CTB), are still present but now appear on conventional spectrum analyzers to be similar to random noise. Thus, to technicians the distortion energy is indistinguishable from random noise. A new digital signal processing (DSP) technique has been developed to process the spectral “noise” in a vacant band to determine if the energy is random, or correlated to a full-band nonlinear distortion signal that could have created it. This paper discusses the processing details of the new test method and presents lab, cascade, and field test results. These data demonstrate the operational benefits of making nonlinear distortion measurements in mostly- or all-digital cable plants.

DISTORTIONS IN CABLE NETWORKS

Active devices through which a cable network’s signals pass compensate for various losses in the transmission path, and extend the physical reach of the network. Unfortunately, those same active devices also degrade the quality of the signals to some extent, with the amount of degradation largely related to the active circuit type (e.g., single-ended, push-pull), the active device’s noise figure, number of signals carried in the network, the number and types of cascaded active devices through which the signals pass, the active devices’ dynamic range, and the active devices’ operating RF levels. The degradation is characterized in terms of parameters such as carrier-to-noise ratio (CNR) and carrier-to-nonlinear distortion ratio. This paper focuses

on nonlinear distortions, in particular the measurement of nonlinear distortions in mostly- or all-digital networks.

Nonlinear distortions

The amplifiers used in cable networks are not perfectly linear devices, that is, their transfer function is not constant. If one were to plot an amplifier’s instantaneous output voltage versus its instantaneous input voltage on a graph (see Figure 1), the resulting line would not be straight.

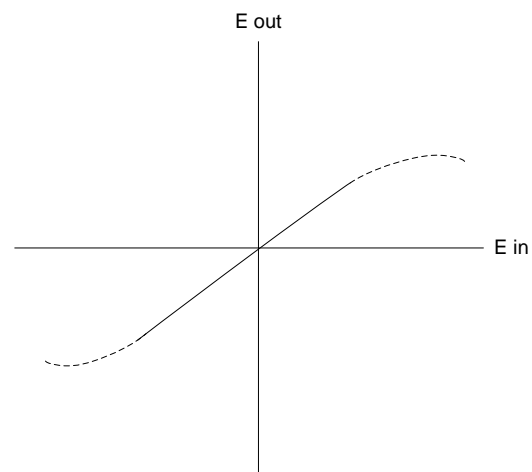


Figure 1. Example plot of amplifier output versus input voltage.

This behavior can be modeled mathematically using a Taylor Series expansion given by the equation

$$f(x) = Ax + Bx^2 + Cx^3 \dots$$

where x is a time-varying input signal, and $f()$ is a nonlinear operator such as an overdriven amplifier (or a cascade of overdriven amplifiers). The A term is linear gain, B is second-order distortion, and C is third order distortion. Higher terms, such as D , E , and F , also may be significant.

In typical operating conditions, the amplifier operates in the linear region (solid line in Figure). In non-ideal operating conditions, such as amplifier failure or overdriving the amplifier into its saturation region, the amplifier starts operating in the nonlinear region (dashed line in Figure 1).

Nonlinear behavior in an amplifier is related in part to small-signal nonlinearities in the amplifier's semiconductor devices, but mostly to signal compression that occurs as the amplifier is operated near its saturation point.

Nonlinear distortions get their name from the nonlinear operation of the amplifier or other active device that creates the distortions. One notable differentiator between linear distortion, such as group delay, and nonlinear distortion is that linear distortion cannot create distortion energy at new frequencies, but nonlinear distortion can. Likewise, as an amplifier's operating signal levels are increased, the relative output ratios of desired carrier levels to distortion levels will be maintained for linear distortion, but will not be maintained for nonlinear distortions.

A graphical illustration of second order nonlinear distortion caused by two signals, F_1 (75 MHz) and F_2 (100 MHz), is shown in Figure 2. Note the discrete distortions or beats at the absolute value of the difference $F_1 - F_2$ (25 MHz), the second harmonic $2F_1$ (150 MHz), the sum of the two frequencies $F_1 + F_2$ (175 MHz), and the second harmonic $2F_2$ (200 MHz).

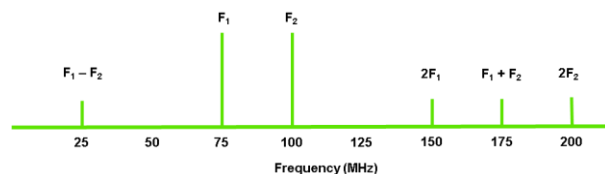


Figure 2. Simplified graphic illustrating discrete second order distortion.

Second and third order distortions

A quick operational test to determine the order of nonlinear distortion in the spectrum is to elevate the amplifier's input signal. If the distortion energy increases 3 dB for a 1 dB step increase of the input signal, the nonlinear distortion is probably third order. If the undesired energy increases 2 dB for a 1 dB step increase of the input signal, the nonlinear distortion is probably second order.

Second order distortion in cable networks should be substantially suppressed relative to third order distortion because cable networks use balanced push-pull amplifiers. Push-pull amplifiers cancel even order (second, fourth, sixth, etc.) distortions. Expected potential sources of abnormal second order distortions are imperfect analog downstream linear lasers; damaged or unbalanced push-pull amplifiers; and distortion caused by diode-like junctions created by corrosion in the plant.

Third order distortion is the dominant nonlinear distortion in cable networks. High-output amplifiers are used to provide needed dynamic range. Cable systems are operated with up-tilt (higher frequencies operated at higher RF output levels than lower frequencies) to provide more uniform distortion over the downstream band. The potential sources mentioned previously for second order distortion also can contribute to third order distortion.

History

In the days of 12-channel operation in North American cable networks, the active devices in the outside plant were single-ended. The nonlinear distortion of concern to most operators was for the most part cross-modulation (XMOD), which, if severe enough, produced a windshield wiper effect in the pictures of analog TV signals. XMOD is a third order distortion.

Since 12-channel cable systems used the same frequencies and channel plan as over-

the-air VHF broadcast television (54 MHz to 88 MHz for channels 2-6, and 174 MHz to 216 MHz for channels 7-13), the discrete second- and some of the third-order nonlinear distortions produced by amplifiers fell in parts of the spectrum where TV signals were not carried.

The introduction of push-pull amplifier technology accommodated more usable channels beyond the 12 VHF broadcast equivalents. The new push-pull actives provided a significant improvement in second order nonlinear distortion performance, so the VHF midband and superband frequency ranges could now be used. That meant an increase in cable network channel capacity.

As the downstream spectrum's upper frequency limit continued to increase with improvements in active and passive device technology over time, so did the number of channels provided by cable operators. Along with increased channel counts were an increase in the numbers of discrete nonlinear distortion products or beats, eventually to the point where it became difficult or impossible to discern individual beats.

Composite distortions

Because of the almost "comb-like" regular frequency spacing of analog TV signals in a cable network using the CEA-542-D channel plan, the resulting distortions cluster at various and predictable frequencies in the spectrum. The individual distortions can be so numerous within each cluster that the descriptor *composite distortion* arguably is more appropriate than *discrete distortion*. CTB distortions of concern cluster in a narrow bandwidth under each visual carrier, and CSO distortion clusters appear ± 0.75 and ± 1.25 MHz relative to the visual carriers.

Nonlinear distortions such as CTB, CSO, and common path distortion (CPD) don't go away in an all-digital network. Rather than clusters of discrete distortions that occur in a

network carrying large numbers of analog TV signals, the nonlinear distortions in a mostly- or all-digital network are noise-like. Those noise-like nonlinear distortion products are known as composite intermodulation noise (CIN), composite intermodulation distortion (CID) or intermodulation noise (IMN) – which should not be confused with thermal noise. (Note: The term composite intermodulation noise and its abbreviation are used in this paper.)

Confusion does occur, though. It is widely-known that raising RF levels in the plant improves the CNR, where "N" is thermal noise. But in a system with a lot of digital signals, raising signal levels improves CNR to a point, then the noise floor starts to *increase* and the CNR appears to get worse.

That seems counterintuitive, but the now-elevated noise floor no longer is just thermal noise. It is a combination of thermal noise and the previously mentioned noise-like nonlinear distortions. When characterizing plant performance in the presence of CIN, the term "carrier-to-composite noise (CCN) ratio" commonly is used.

Indeed, CCN is a much more appropriate measurement metric than is CNR under these circumstances, because there is no practical way to differentiate thermal noise from CIN on a spectrum analyzer display. One could turn off all downstream signals except for automatic gain control/automatic level control (AGC/ALC) pilot(s); the noise-like nonlinear distortions would go away, leaving just thermal noise. Unfortunately, this method is service disruptive, and as such is not a practical way to characterize noise versus noise-like nonlinear distortions.

How, then, can nonlinear distortions in a mostly- or all-digital network be measured in an operating network?

Characterizing noise-like nonlinear distortion

Noise-like nonlinear distortion energy is not random, and can be quantified with knowledge of the input signal that created it. It is particularly easy to quantify in vacant test bands, such as a roll-off region. If a vacant band is not available, one can be created by demodulating the RF signal occupying the band, and then subtracting it mathematically.

There are a few possible ways that detection of signal distortion can be done. One method is to capture the same signal twice: One copy of which is a clean undistorted signal at the headend or hub site, and the other copy is captured at a test point in the field. This method has the added complexity of requiring synchronized capture and the transfer of data to a central processing point, in addition to removing linear distortion differences between the nonlinearly distorted signal and the pristine headend signal.

Another method involves capturing the signal at the input and the output test points of an amplifier, and then determining how much additional distortion was added by the amplifier. The linear distortion of the amplifier, including diplex filters response, tilt, and equalization makes this method non-trivial.

The next section of this paper describes a test methodology that requires only a signal capture at one location, where the single full band signal is captured in the field. The captured vacant band signal is stored as a “measured” signal, and processed with a “manufactured” signal. The level of match between the measured and manufactured signals determines how much nonlinear distortion was present in the captured signal’s vacant band.

ONE-SIGNAL NONLINEAR DISTORTION TEST METHOD

The following steps can be used to facilitate a one-signal nonlinear distortion

measurement, using just the signal captured in the field.

1) Capture a full-band downstream signal (the entire downstream RF spectrum with all signals and vacant bands) using a digital oscilloscope that has a sampling rate of at least twice the bandwidth of the downstream band, and 10-12 bits of analog-to-digital (A-D) resolution for at least 32,768 samples. In our example, the downstream bandwidth is less than 1,250 MHz, thus the downstream signal is digitized at a rate of at least 2.5×10^9 Hz. If necessary, a low-distortion, low-noise preamplifier can be used to boost the full band downstream signal prior to capture (digital oscilloscopes generally have a poor noise figure). A low pass filter should be used to remove any energy above 1250MHz, to prevent aliasing. Figure 3 illustrates a time domain display of a signal captured by a digital oscilloscope operating at 2.5 gigasamples per second and 12 bits of A-D resolution. The downstream signal processing requires a vacant band, which may be a roll-off band. This example 54 MHz to 860 MHz

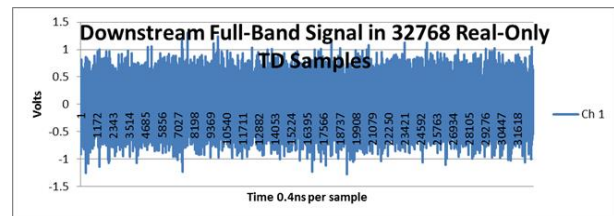


Figure 3. Captured time domain signal comprising 32768 samples, and with a duration of 16.384 μ s.

signal comprised mostly digital signals, plus a few continuous wave (CW) carriers used as pilots and alignment aids. The captured signal contains a vacant band between about 770 MHz and 860 MHz, which is not evident in the time domain trace.

2) Convert the time domain signal of Figure 3 into the frequency domain with a fast Fourier transform (FFT). The resulting frequency domain plot is illustrated in Figure 4. In the frequency domain, the vacant band energy values between 770 MHz and 860 MHz are

cut and stored. These frequency domain

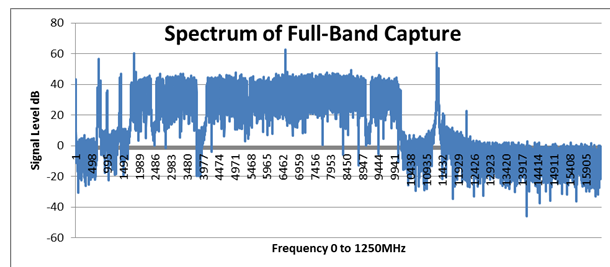


Figure 4. Full bandwidth downstream frequency domain signal obtained by performing an FFT on the time samples shown in Figure 3.

samples are called the “measured” vacant band distortion signal. Next, replace the vacant band energy in the frequency domain signal between 770 MHz and 860 MHz with zeroes. This spectral plot is illustrated in Figure 5.

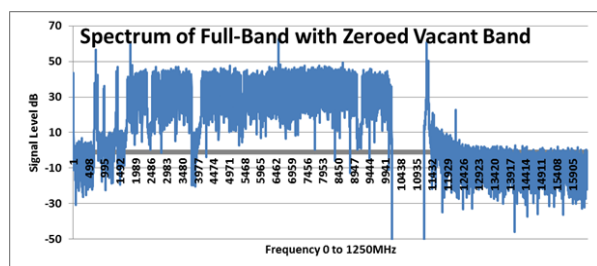


Figure 5. Full bandwidth downstream display with vacant band zeroed out.

3) Next, convert the 54 MHz to 860 MHz signal of Figure 5 with the newly-vacated band back into the time domain with an inverse fast Fourier transform (IFFT), and distort a resulting time sequence with a second and third order nonlinear distortion.

The latter is accomplished by squaring and cubing each term in the time sequence. This creates a second order “manufactured” signal and a third order “manufactured” signal. This distortion manufacturing method gives a good approximate estimate because the nonlinear distortion components are small in operating cable networks. That is:

$$f(x) = Ax + Bx^2 + Cx^3 \sim Ax$$

4) Convert the “manufactured” signals back into the frequency domain and store only the distortion components in the vacant band (770 MHz to 860 MHz in our example).

5) Process the vacant band “measured” signal with the vacant band “manufactured” signals. One processing method that has worked well is frequency domain division of the “manufactured” samples, illustrated in Figure 8, by the complex conjugate of the same frequency “measured” samples, illustrated in Figure 9, to produce frequency domain quotients.

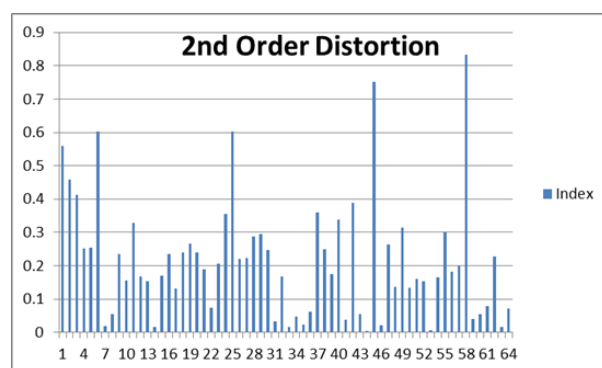


Figure 6. Time domain plot of quotient showing average first term relative to other terms, indicating low second order distortion.

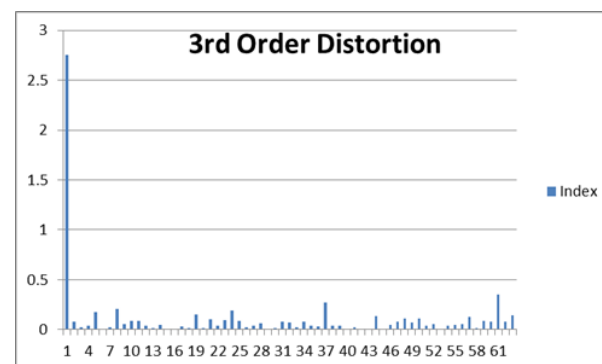


Figure 7. Time domain plot of quotient showing large first term relative to other terms, indicating third order distortion.

6) Convert the 1024 frequency domain quotients into the time domain. This is illustrated in Figure 6 for second order distortion and Figure 7 for third order distortion. Energy in the first (DC) term

indicates a match of the “measured” signal with the “manufactured” signal.

7) If necessary, averaging may be used to better discern the DC term relative to the other terms. Note that the DC terms are correlated vectors that will add, but the other terms are uncorrelated.

8) Repeat the previous steps for other orders of distortion that might be present.

The plots of Figure 6 and Figure 7 are complex time series, and only 64 sample

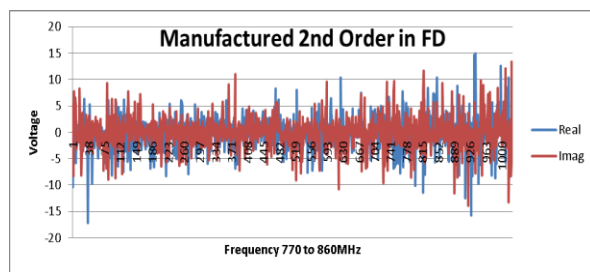


Figure 8. Sample points of manufactured second order distortion from the vacant band.

points are illustrated. As the number of averages increases, the noisy components associated with using a noise-like downstream test signal are reduced. Another improvement to reduce noise in the plots is to use a larger percentage of vacant bandwidth relative to the occupied bandwidth. There is generally a angle to the distortion, and in most observed tests on distorted cable amplifiers, the first term ($t = 0$) contains most of the energy. As the amplifier’s input drive level increases, both the level of nonlinear distortion and the

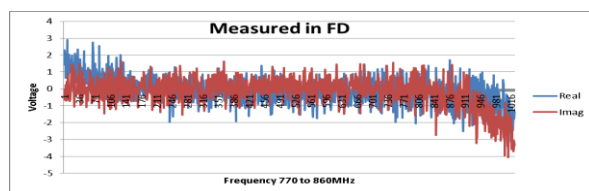


Figure 9. Sample points of measured distortion from the vacant band.

angle of the DC terms change.

OUTSIDE PLANT TESTING

Test Results Obtained from Testing Inside Houses

Figure 10 is a composite plot from seven different locations for second order distortion test results, and Figure 1 contains third order distortion results. Fifteen separate tests were conducted to determine if the measurements were repeatable, and 10 averages used for each point. Locations 6 and 7 had downstream high pass filters to block all but the data-only traffic. Note the top trace on the second order distortion Figure 10, which was location 3. This particular location was later diagnosed also have high linear distortion, as determined by ripples in the upstream equalization response.

The .750 trunk cable feeding this location appeared to have been damaged when it was installed many years ago. In the photograph of Figure 12, one can make out the conduit which may have been fractured by a boring machine. The cable was severely kinked several feet below ground and corroding as one would expect. After repair both the second and third order distortion improved significantly.

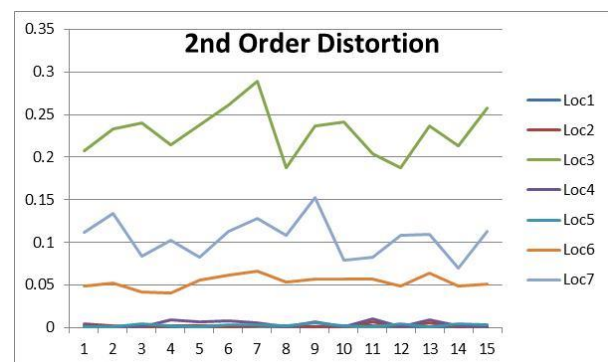


Figure 10. Second order results for seven locations (15 tests each location, 10 averages)

The highest third order distortion came from a home with known ingress issues.

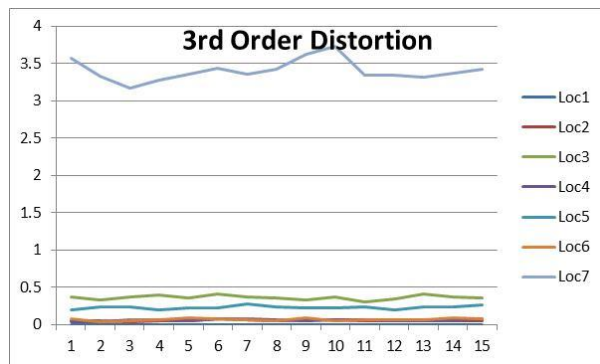


Figure 11. Third order results for seven locations (15 tests each location, 10 averages)



Figure 12. The kinked corroding cable causing the high second order distortion for location 3.

Test Results Obtained from Testing a Node Plus 6 Amplifier Cascade

Tests were performed on a cascade of node plus six push pull amplifiers. The amplifiers were capable of 860 MHz but were only loaded to 770 MHz, so testing was done in the vacant band between 770 MHz and 860 MHz, as described previously. Loading was with digital carriers.

Figure 13 shows the test results for second and third order distortion. Note that the third order nonlinear distortion increased through the third amplifier as expected, but then began to decrease. At amplifiers 6 and 7 the nonlinear third order distortion took a precipitous drop. Second order distortion was not significant. Note, too, that the worst

second order distortion was observed at the fiber node.

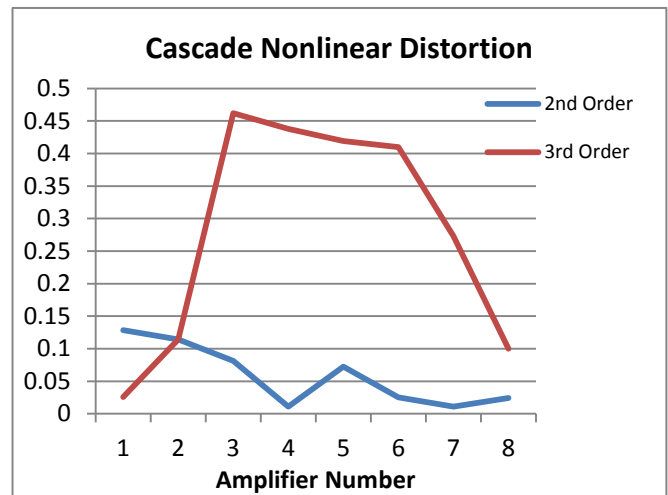


Figure 13. Distortion changes in a cascade of node plus seven amplifiers

This observed third order behavior is not understood at this time. One possible explanation is distortion cancellation by inadvertent addition out-of-phase distortion (a.k.a. predistortion). This method is used commercially in high power amplifiers to extend their dynamic ranges, but the authors are not aware of this being done in cable TV-type distribution amplifiers. Testing additional cascades will hopefully be done in the future to determine whether what was seen here was an anomaly.

LAB TESTING

Lab-based testing was conducted to validate the nonlinear distortion measurement concept discussed in this paper. A single-ended amplifier (Agilent 8447D) and a 54 MHz to 860 MHz cable push-pull hybrid amplifier (ATX model QDAXU) were used in the lab tests.

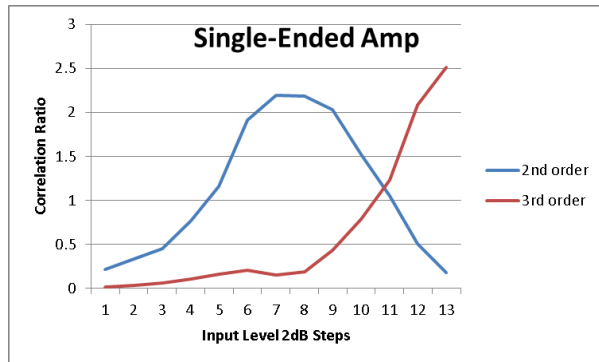


Figure 14. Single-ended amplifier performance.

The input signal was a broadband random noise source (NoiseCom UFX 7109) with its RF output filtered using a 600 MHz low pass filter (Mini-Circuits model BLP-600-75) to create a vacant test band around 800 MHz. The ratio of the energy in the DC term of the correlation plot to all other correlation coefficients was plotted versus input drive level as the input drive level was increased in 2 dB steps. Figure 14 shows that the single-ended amplifier first exhibited an increase in 2nd order distortion, followed by an increase in 3rd order distortion at higher input drive levels. Of interest was the second order distortion decreasing with heavy saturation levels.

Figure 15 shows the same plots for the push-pull cable downstream amplifier. The second order distortion remains low for all drive levels, while the third order distortion increases with higher drive levels.

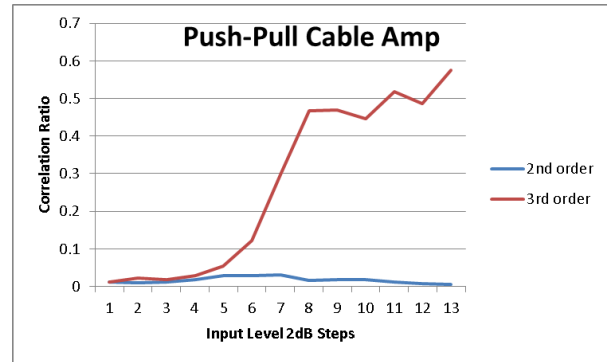


Figure 15. Push-pull amplifier performance.

RETURN PATH TESTING

The nonlinear distortion measurement method described in this section was demonstrated at the CableLabs 2014 Winter Conference. This new method was developed to analyze RF signals to determine the presence of nonlinear distortion using digital signal processing techniques. The method involves multiple transmissions of a burst (or a known variant of the burst), and performing a full-band signal capture containing a vacant band having noise and/or distortion for each transmission. As described here, it is possible to use this measurement method to evaluate a cable network's return spectrum, although it also could be used for other applications, such as wireless transmitters.

The energy in the vacant band from the first burst transmission in Figure 18 is processed with the energy in the vacant band from the subsequent transmissions in Figure 18 to see the correlation between the two energies. Figure 16 shows the mid-split 5 MHz to 85 MHz upstream burst test signals

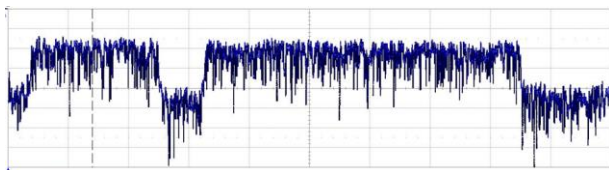


Figure 16. Full band capture for upstream signal with a vacant band.

with a vacant band 25 MHz to 35 MHz, where the energies were processed and analyzed. In situations where there is no nonlinear distortion occurring in the network, the signal in the vacant band is expected to be white Gaussian noise, and thus the energy captures in the vacant band from the multiple transmissions are expected to be uncorrelated. When nonlinear distortion does occur in the network, the signal in the vacant band is expected to contain distortion components from the transmitted signal; the energy levels of the distortion components in the vacant bands are directly related to the amount of

distortion occurring in the network. In these situations, the energy captures in the vacant band from the multiple transmissions are expected to have a certain level of correlation.

By correlating the energy captures in the vacant band, detection of non-linear distortion is possible. Figure 17 shows the result from correlating (using frequency domain processing) the vacant band energy captures for two identical time-separated bursts sent

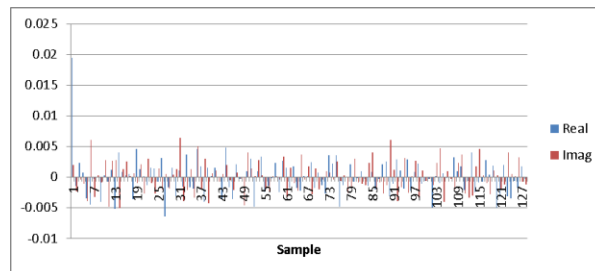


Figure 17. Correlation plot of vacant band energy from two identical bursts.

through a network suffering from nonlinear distortion. The presence of a large DC term in the correlation plot is indicative of the presence of nonlinear distortion.

As mentioned previously, the transmitted bursts are sent in sequence, and are either identical, or the subsequent bursts could be a variant of the original burst. One option would be to transmit a second identical burst and the third burst as an inverted version of the original burst as is shown in Figure 18.

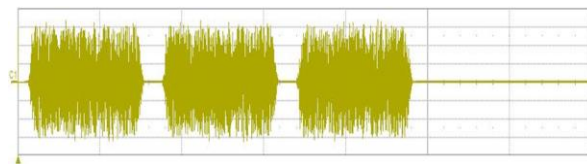


Figure 18. Multiple burst transmission in time domain: identical first and second bursts, identical but inverted third burst.

Transmission of the third inverted burst enables the identification of odd-ordered distortion in the network such as CTB.

To detect CTB (or odd-ordered distortion), the correlation results of the

vacant band energy of the first burst and the second burst are compared to the correlation results of the vacant band energy of the first (or second) burst and the third burst. If the correlation results from the inverted burst go negative, it is indicative of odd-ordered distortion.

These test methods can potentially be incorporated into digital terminals and CMTSs, so that testing can be performed remotely without the need for a truck roll. Patent pending.

SUMMARY

This paper discussed nonlinear distortions in cable networks and methods to discriminate nonlinear distortion from thermal noise in all-digital networks. One method is appropriate for downstream signals which are continuous transmissions, and another method is for upstream transmissions, which are generally bursty. With these new test methods, cable operators can potentially move to new levels of plant fault detection.

REFERENCES

Broadband Cable Access Networks, by David Large and James Farmer (© 2009, Morgan Kaufmann Publishers, ISBN 978-0-12-374401-2)

Code of Federal Regulations, Title 47, Part 76

Modern Cable Television Technology, 2nd Edition, by Walter Ciciora, James Farmer, David Large, and Michael Adams (© 2004, Morgan Kaufmann Publishers, ISBN 1-55860-828-1)

SCTE Measurement Recommended Practices for Cable Systems, Fourth Edition, (© 2012, Society of Cable Telecommunications Engineers, TS46)

ACKNOWLEDGMENTS:

The authors wish to express their gratitude for access and support to the cable operators that supported research for this paper.